J. Fluid Mech. (2013), *vol.* 720, *pp.* 618–636.
doi:10.1017/jfm.2013.2

The trailing vorticity field behind a line source in two-dimensional incompressible linear shear flow

Sjoerd W. Rienstra[1],†, Mirela Darau[1,2] and Edward J. Brambley[3]

[1]Department of Mathematics and Computer Science, TU Eindhoven, Den Dolech 2, 5612 AZ Eindhoven, The Netherlands

[2]Department of Mathematics and Computer Science, WU of Timişoara, Blvd. V. Parvan 4, Timisoara 300223, Romania

[3]Department of Applied Mathematics and Theoretical Physics, University of Cambridge, Wilberforce Road, Cambridge CB3 0EW UK

(Received 18 December 2011; revised 21 July 2012; accepted 22 December 2012)

The explicit exact analytic solution for harmonic perturbations from a line mass source in an incompressible inviscid two-dimensional linear shear is derived using a Fourier transform method. The two cases of an infinite shear flow and a semi-infinite shear flow over an impedance boundary are considered. For the free-field and hard-wall configurations, the pressure field is (in general) logarithmically diverging and its Fourier representation involves a diverging integral that is interpreted as an integral of generalized functions; this divergent behaviour is not present for a finite impedance boundary or if the frequency equals the mean flow shear rate. The dominant feature of the solution is the hydrodynamic wake caused by the shed vorticity of the source. For linear shear over an impedance boundary, in addition to the wake, (at most) two surface modes along the wall are excited. The implications for duct acoustics with flow over an impedance wall are discussed.

Key words: aeroacoustics, general fluid mechanics, vortex shedding

1. Introduction

The sound field from a mass point source in a cylindrical duct with a uniform centre part of the mean flow and finite linearly varying boundary layers (as studied in Brambley, Darau & Rienstra 2012), formulated in the form of a spatial Fourier integral, has been shown to consist of modes (residues of the Fourier transform) and the contribution from a branch cut. Some of the modes are purely acoustical and disappear with increasing sound speed, and some are hydrodynamical, including some surface waves related to the impedance wall, one of which is an instability due to the interaction between the boundary layer, mean flow and impedance wall.

Of particular interest is the fact that if the source is inside the boundary layer, there is a pole along the branch cut, triggering a non-modal contribution. This field is not present when the mass source is within a uniform flow region, and it is therefore not a normal mode, of which the existence is independent of the source.

† Email address for correspondence: s.w.rienstra@tue.nl

The calculation of this contribution, and the contribution of the branch cut as a whole, is determined in Brambley *et al.* (2012) numerically. In the present paper an analytical form is obtained in the incompressible limit which provides some useful insights into the behaviour and properties of this contribution.

On the other hand, the present results are of wider interest. In studies of the related problem of a Green's function in a free mixing layer (Suzuki & Lele 2003*a*), a boundary layer along a wall (Suzuki & Lele 2003*b*), and a non-uniform jet flow (Goldstein & Leib 2005, and other references therein), the solutions were formulated by a similar spatial Fourier representation, but this non-modal contribution was either not explicitly mentioned or was overlooked during approximation. Yet, as we will now see, there must be one in any situation involving a mass source in sheared flow.

This non-modal contribution is here identified as a wake, non-acoustic and hydrodynamic in nature, due to the shed vorticity of the mass source, which is analogous to the phenomenon of vortex stretching. In linear theories of perturbations of relatively simple mean flows, this vortex shedding is well known from an external force, but it is not common from mass sources.

Consider the equations for conservation of mass and momentum in an inviscid flow with density ρ, pressure p, velocity $\boldsymbol{v}$, and a mass source Q and bulk force $\boldsymbol{F}$,

$$\frac{\partial \rho}{\partial t} + \boldsymbol{\nabla} \cdot (\rho \boldsymbol{v}) = Q, \quad \rho \frac{\partial \boldsymbol{v}}{\partial t} + \rho(\boldsymbol{v} \cdot \boldsymbol{\nabla})\boldsymbol{v} + \boldsymbol{\nabla} p = \boldsymbol{F}. \tag{1.1}$$

In a barotropic fluid (for example a homentropic or incompressible fluid) we have from the curl of the momentum equation the following equation for vorticity $\boldsymbol{\omega} = \boldsymbol{\nabla} \times \boldsymbol{v}$:

$$\frac{\partial \boldsymbol{\omega}}{\partial t} + \boldsymbol{v} \cdot \boldsymbol{\nabla}\boldsymbol{\omega} = \boldsymbol{\omega} \cdot \boldsymbol{\nabla}\boldsymbol{v} - \boldsymbol{\omega}\boldsymbol{\nabla} \cdot \boldsymbol{v} + \boldsymbol{\nabla} \times (\boldsymbol{F}/\rho), \tag{1.2}$$

or, by using the mass equation,

$$\rho \left(\frac{\partial}{\partial t} + \boldsymbol{v} \cdot \boldsymbol{\nabla} \right) \left(\frac{\boldsymbol{\omega}}{\rho} \right) = \boldsymbol{\omega} \cdot \boldsymbol{\nabla}\boldsymbol{v} - \frac{\boldsymbol{\omega}}{\rho} Q + \boldsymbol{\nabla} \times (\boldsymbol{F}/\rho), \tag{1.3}$$

where $\boldsymbol{\omega} \cdot \boldsymbol{\nabla}\boldsymbol{v}$ is called the vortex stretching term (Tennekes & Lumley 1972, p. 83; Kundu & Cohen 2002, p. 139). This term stretches and tilts the vortex lines, changing the local vorticity. Altogether we may conclude from (1.3) that the vorticity of a particle changes either by stretching, by a mass source (provided $\boldsymbol{\omega} Q \neq 0$), or by a non-conservative external force field. This shows that the presence of a mass source in a region of sheared flow, as in Brambley *et al.* (2012) but indeed also in Suzuki & Lele (2003*a*,*b*) and Goldstein & Leib (2005), necessarily causes a trailing vorticity field.

In two dimensions the stretching term vanishes because there is no velocity component in the direction of $\boldsymbol{\omega}$. So a particle's vorticity can only change by an external force or mass source. If $\boldsymbol{\nabla} \times (\boldsymbol{F}/\rho) = 0$ we have for χ, where $\boldsymbol{\omega} = \chi \boldsymbol{e}_z$, the conservation equation

$$\frac{\partial \chi}{\partial t} + \boldsymbol{\nabla} \cdot (\boldsymbol{v}\chi) = 0 \tag{1.4}$$

affirming the classic result that (without a non-conservative external force) in two dimensions vorticity χ is conserved. So if the vorticity of a particle changes due to a mass source, it can only be a redistribution because there is no vorticity production.

If the problem of interest relates to linear perturbations of an irrotational mean flow (i.e. with vanishing mean vorticity), caused by a small force or source field, the only source of (linear) vorticity can be the force, because the product $\boldsymbol{\omega}Q$ is quadratically small. If, however, the mean vorticity is non-zero, the mass source too may produce (redistribute) vorticity perturbations.

This is what we will study here in a very simplified and idealized model problem, allowing exact solutions. Therefore we will assume in the following that $\boldsymbol{F} = 0$. It should be noted that to a large degree this is a modelling assumption, although possibly a point heating, such as from a laser, may be a viable physical example of a mass source, or at least a volume source, of the type considered here.

When we return to the two-dimensional vorticity equation (now without the force term)

$$\rho\left(\frac{\partial}{\partial t} + \boldsymbol{v}\cdot\boldsymbol{\nabla}\right)\left(\frac{\chi}{\rho}\right) = -\frac{\chi}{\rho}Q \tag{1.5}$$

and assume that a small source induces harmonic isentropic perturbations to a parallel sheared flow U with otherwise constant density ρ_0 and sound speed c_0 given by

$$\boldsymbol{v} = U(y)\boldsymbol{e}_x + \hat{\boldsymbol{v}}\mathrm{e}^{\mathrm{i}\omega t}, \quad \chi = -U'(y) + \hat{\chi}\mathrm{e}^{\mathrm{i}\omega t}, \quad \rho = \rho_0 + c_0^{-2}\hat{p}\mathrm{e}^{\mathrm{i}\omega t}, \quad Q = \hat{q}\mathrm{e}^{\mathrm{i}\omega t}, \tag{1.6}$$

we have

$$\rho_0\left(\mathrm{i}\omega + U(y)\frac{\partial}{\partial x}\right)\left(\hat{\chi} + \frac{U'(y)}{\rho_0 c_0^2}\hat{p}\right) = U'(y)\hat{q}. \tag{1.7}$$

With a monopole-type line source of amplitude $2\pi S$ (we will use the term line source in two dimensions for what is really a line source in three dimensions along the third dimension)

$$\hat{q} = 2\pi S\delta(x)\delta(y) \tag{1.8}$$

(where $\delta(\ )$ denotes the delta function) and abbreviations $U(0) = U_0$, $U'(0) = \sigma$, we have

$$\rho_0\left(\mathrm{i}\omega + U(y)\frac{\partial}{\partial x}\right)\left(\hat{\chi} + \frac{U'(y)}{\rho_0 c_0^2}\hat{p}\right) = 2\pi S\sigma\,\delta(x)\delta(y) \tag{1.9}$$

which has, under causal free-field conditions (allowing only perturbations generated by the source) and $U_0 > 0$, the solution

$$\hat{\chi} + \frac{\sigma}{\rho_0 c_0^2}\hat{p} = \frac{2\pi S\sigma}{\rho_0 U_0}H(x)\mathrm{e}^{-\mathrm{i}k_0 x}\delta(y), \quad k_0 = \frac{\omega}{U_0}, \tag{1.10}$$

where $H(x)$ is Heaviside's step function. Noting that the pressure term in (1.10) cannot be discontinuous, we see that this simple derivation shows that a line source in shear flow produces a semi-infinite sheet of vorticity, undulating with hydrodynamic wavenumber k_0. (Note that if the mean flow is unstable, for example if the profile has an inflection point, this solution will probably not exist in reality without exciting the unstable modes.)

This vortex shedding was observed in the acoustic problem of a (circumferential Fourier component of a) point source in the linearly sheared boundary layer of a mean flow in a duct (Brambley *et al.* 2012). In the present paper we will show that this phenomenon is not essentially acoustical but more generally of hydrodynamic nature.

We consider the effect of a time-harmonic line mass source on an incompressible inviscid two-dimensional shear flow of infinite (§ 2) or semi-infinite (§ 3) extent. The

semi-infinite configuration concerns a shear flow along an impedance wall, including its hard-wall limit. This problem is in many respects similar to the infinite shear case, since there is again the vorticity trailing from the source, but at the same time the interaction with the wall is more subtle.

In order to derive exact expressions for pressure and velocity, we will assume a linearly sheared mean flow, so with a uniform mean flow vorticity. This is a simplification valid in a (relatively) thick boundary layer, for example the atmospheric boundary layer or down the bypass duct of an turbofan aero-engine. Although the shear is obviously created by viscous forces, the present problem is effectively inviscid if we assume that the Reynolds numbers related to the relevant length scales (hydrodynamic wavelength $2\pi/k_0$, velocity–shear ratio U/U') are large. For a discussion of possible effects of viscosity, including analytical results, see Wu (2002, 2011).

The exact analytic solutions obtained appear to be new, in spite of this rather simple configuration, with the nearest known solutions being the velocity field given in Balsa (1988) and Criminale & Drazin (1990, 2000) for the initial value problem of a line source in a linear shear layer.

As far as the vorticity component is concerned, the problem is already solved by (1.10). As the fluid is assumed incompressible, the factors proportional to $1/c_0^2$ reduce to zero and (1.10) gives the vorticity as

$$\hat{\chi} = \frac{2\pi S\sigma}{\rho_0 U_0} H(x)\mathrm{e}^{-\mathrm{i}k_0 x}\delta(y). \tag{1.11}$$

The solutions for pressure and velocities are not so simple, as they have to satisfy boundary conditions. Here, they are found by Fourier transformation in x, as this approach is most flexible and versatile, and can be utilized for both free-field and impedance wall configurations to obtain the velocities as well as the pressure. In the free-field problem, the velocities can also be obtained by a more direct integration of a Greens function representation, but this approach does not seem to be as convenient as Fourier transformation.

There is a catch however: the pressure field of a two-dimensional source without mean flow diverges like $\log(x^2+y^2)$ for large x^2+y^2, and the same appears to happen in linear shear flow if the frequency ω is not equal to the mean flow shear rate σ. As a result, the pressure solutions for the free-field and the hard-wall configurations are not classically Fourier transformable, although the impedance wall solution is found not to share this divergent behaviour. We will circumvent this problem by considering the divergent Fourier integral of the pressure in the context of generalized functions (Jones 1982) and carefully subtract the singular part. The result is then only unique up to addition of an undetermined constant. This, however, is expected, as the pressure in an incompressible model with free-field or hard-wall boundary conditions appears only in the form of its gradient and is therefore only defined up to a (time-dependent) constant.

From an acoustic perspective we can understand this divergence also in another way. This incompressible field is the inner solution, valid in a region $\sqrt{x^2+y^2} \ll O(c_0/\omega)$, of a small-Helmholtz-number approximation of matched-asymptotic-expansion type in much the same way as in Wu (2002, § 5). See also Lesser & Crighton (1975) and Crighton *et al.* (1992). Therefore, the diverging source field is just the leading log-term of the small-argument expansion of an outer solution of $H_0^{(2)}(\omega\sqrt{x^2+y^2}/c_0)$-type.

2. A time-harmonic line mass source in infinite linear shear

2.1. *Free-field solution*

Consider the two-dimensional incompressible inviscid model problem of perturbations of a linearly sheared mean flow due to a time-harmonic line source at $x = y = 0$ with time dependence $\mathrm{e}^{\mathrm{i}\omega t}$:

$$\rho_0\left(\frac{\partial u}{\partial x}+\frac{\partial v}{\partial y}\right)=2\pi S\delta(x)\delta(y), \tag{2.1a}$$

$$\rho_0\left(\mathrm{i}\omega+U\frac{\partial}{\partial x}\right)u+\rho_0\frac{\mathrm{d}U}{\mathrm{d}y}v+\frac{\partial p}{\partial x}=0, \tag{2.1b}$$

$$\rho_0\left(\mathrm{i}\omega+U\frac{\partial}{\partial x}\right)v+\frac{\partial p}{\partial y}=0. \tag{2.1c}$$

The far-field boundary conditions will be of vanishing velocity, but (as we will see) not of vanishing pressure. Another point to be noted here, as it will be important later, is that the pressure appears only as a spatial gradient, and so will necessarily only be determined up to a (time-dependent) constant.

After Fourier transformation in x we obtain the following set of equations:

$$\rho_0(-\mathrm{i}k\tilde{u}+\tilde{v}')=2\pi S\delta(y),\quad \mathrm{i}\rho_0\Omega\tilde{u}+\rho_0U'\tilde{v}-\mathrm{i}k\tilde{p}=0,\quad \mathrm{i}\rho_0\Omega\tilde{v}+\tilde{p}'=0, \tag{2.2}$$

where $\Omega=\omega-kU$ and the prime denotes a derivative to y. This system may be further reduced to an incompressible form of the Pridmore-Brown (1958) equation by eliminating $\tilde{v}$ and $\tilde{u}$, which, upon considering a doubly infinite linear shear flow with $U(y)=U_0+\sigma y$ and $\Omega_0=\omega-kU_0$, becomes

$$\tilde{p}''+\frac{2k\sigma}{\Omega}\tilde{p}'-k^2\tilde{p}=-2\pi\mathrm{i}S\Omega_0\delta(y). \tag{2.3}$$

The boundary conditions will be a decaying field at infinity, although that will be strictly possible only for the velocity; the pressure will at best be slowly diverging.

The homogeneous equation has two independent solutions $\mathrm{e}^{\pm ky}(\Omega\pm\sigma)$ (Rayleigh 1945, p. 368; Drazin & Reid 2004, p. 146), or

$$\tilde{p}_1(y)=\mathrm{e}^{|k|y}(\Omega+\operatorname{sign}(\operatorname{Re}k)\sigma),\quad \tilde{p}_2(y)=\mathrm{e}^{-|k|y}(\Omega-\operatorname{sign}(\operatorname{Re}k)\sigma), \tag{2.4}$$

where

$$|k|=\operatorname{sign}(\operatorname{Re}k)k=\sqrt{k^2}, \tag{2.5}$$

where $\sqrt{\ }$ denotes the principal-value square root, and $|k|$ has thus branch cuts along $(-\mathrm{i}\infty,0)$ and $(0,\mathrm{i}\infty)$. Note that neither of these solutions has a log-like singularity or requires a branch cut in the complex-y plane. The Wronskian is

$$W(y;k)=\tilde{p}_2'(y)\tilde{p}_1(y)-\tilde{p}_1'(y)\tilde{p}_2(y)=-2|k|\Omega^2, \tag{2.6}$$

and the Fourier-transformed solution is thus

$$\tilde{p}(y,k)=\frac{\mathrm{i}\pi S}{|k|\Omega_0}\mathrm{e}^{-|ky|}(\Omega\Omega_0-\sigma^2|ky|-\sigma^2). \tag{2.7}$$

The physical field in the x,y-domain is hence obtained by inverse Fourier transformation:

$$p(x,y)=\frac{1}{2\pi}\int_{-\infty}^{\infty}\tilde{p}(y,k)\mathrm{e}^{-\mathrm{i}kx}\,\mathrm{d}k=\frac{1}{2}\mathrm{i}S\int_{-\infty}^{\infty}\frac{\mathrm{e}^{-\mathrm{i}kx-|ky|}}{|k|\Omega_0}(\Omega\Omega_0-\sigma^2|ky|-\sigma^2)\,\mathrm{d}k, \tag{2.8}$$

which has singularities at $k = 0$ (if $\omega^2 \neq \sigma^2$) and at $k = k_0 = \omega/U_0$ from $\Omega_0 = -U_0(k - k_0) = 0$. Folding the contour around the branch cuts of $|k|$ (upwards if $x < 0$ and downwards if $x > 0$) to obtain the steepest descent contour, while noting from (1.11) that the contribution of the k_0 pole is the downstream trailing vorticity of the line source, we obtain

$$p(x, y) = \frac{\pi S\sigma^2}{\omega}(1 + k_0|y|)H(x)\mathrm{e}^{-\mathrm{i}k_0 x - k_0|y|} + \mathrm{i}S\int_0^\infty \frac{\mathrm{e}^{-\lambda|x|}}{\lambda\Omega_0^\pm}\left[(\Omega^\pm\Omega_0^\pm - \sigma^2)\cos\lambda y - \sigma^2\lambda y\sin\lambda y\right]\mathrm{d}\lambda \tag{2.9}$$

where $\Omega^\pm = \omega \pm \mathrm{i}\lambda U$ and $\pm = \mathrm{sign}(x)$.

The singularity at $k = 0$ is, unlike the one at k_0, not a pole and has a different origin. Due to this singularity the Fourier representation of the pressure is too singular to be interpreted normally. This is caused by p being not Fourier transformable, not because p itself is singular. As mentioned before, (if $\omega^2 \neq \sigma^2$) p diverges as $\sim\log(x^2 + y^2)$ for $x^2 + y^2 \to \infty$ and is hence not integrable. This is an artefact of the model, including an infinite line source in an incompressible medium. When we consider the incompressible problem as an inner problem of a larger compressible problem, as in Lesser & Crighton (1975), Crighton *et al.* (1992) and Wu (2002), this divergent behaviour disappears as it changes in the far field into an outward radiating acoustic wave.

The inverse Fourier integral, however, can be found if the singular integral is interpreted in the generalized sense, and the singular part is split off. Following Jones (1982, p. 105), we change the semi-infinite integral into a doubly infinite one by replacing $1/\lambda$ by the generalized function

$$\lambda^{-1}H(\lambda) = \frac{\mathrm{d}}{\mathrm{d}\lambda}H(\lambda)\log|\lambda|. \tag{2.10}$$

After integration by parts we obtain the convergent integrals

$$p(x, y) = \frac{\pi S\sigma^2}{\omega}(1 + k_0|y|)H(x)\mathrm{e}^{-\mathrm{i}k_0 x - k_0|y|} - \mathrm{i}S\int_0^\infty \log\lambda\frac{\mathrm{d}}{\mathrm{d}\lambda}\left[\mathrm{e}^{-\lambda|x|}\Omega^\pm\cos\lambda y\right]\mathrm{d}\lambda + \mathrm{i}S\sigma^2\int_0^\infty \log\lambda\frac{\mathrm{d}}{\mathrm{d}\lambda}\left[\mathrm{e}^{-\lambda|x|}\frac{\cos\lambda y + \lambda y\sin\lambda y}{\Omega_0^\pm}\right]\mathrm{d}\lambda. \tag{2.11}$$

Each one can be integrated as follows:

$$\int_0^\infty \log\lambda\frac{\mathrm{d}}{\mathrm{d}\lambda}\left[\mathrm{e}^{-\lambda|x|}\Omega^\pm\cos\lambda y\right]\mathrm{d}\lambda = \omega\gamma + \tfrac{1}{2}\omega\log(x^2 + y^2) - \mathrm{i}U\frac{x}{x^2 + y^2}, \tag{2.12a}$$

$$\omega\int_0^\infty \log\lambda\frac{\mathrm{d}}{\mathrm{d}\lambda}\left[\mathrm{e}^{-\lambda|x|}\frac{\cos\lambda y + \lambda y\sin\lambda y}{\Omega_0^\pm}\right]\mathrm{d}\lambda = \gamma + \tfrac{1}{2}\log(x^2 + y^2) + \tfrac{1}{2}(1 - k_0 y)E(k_0, z) + \tfrac{1}{2}(1 + k_0 y)E(k_0, \bar{z}), \tag{2.12b}$$

where $z = x + \mathrm{i}y$, $\gamma = 0.5772156649\ldots$ is Euler's constant and $E(k_0, z) = \mathrm{e}^{-\mathrm{i}k_0 z}E_1(-\mathrm{i}k_0 z)$, with E_1 the exponential integral with (here) the standard branch cut along the negative real axis of its argument. This results for $E_1(-\mathrm{i}k_0 z)$ in a branch cut along the line $x = 0, y > 0$ and for $E_1(-\mathrm{i}k_0\bar{z})$ in a branch cut along the

line $x=0, y<0$ (see the Appendix, (A 3)). Altogether, we have

$$p(x,y) = -S(U_0+\sigma y)\frac{x}{x^2+y^2} + \frac{\mathrm{i}S}{\omega}(\sigma^2-\omega^2)\left[\gamma + \tfrac{1}{2}\log(x^2+y^2)\right] + \frac{\mathrm{i}S\sigma^2}{2\omega}[(1-k_0y)E(k_0,z) + (1+k_0y)E(k_0,\bar{z}) - 2\pi\mathrm{i}(1+k_0|y|)H(x)\mathrm{e}^{-\mathrm{i}k_0x-k_0|y|}]. \tag{2.13}$$

A seemingly different result would have been obtained if we had scaled λ by a positive factor. The above regularization of the divergent integral would have produced, via the logarithm, a result that differs by a constant. This, however, is entirely to be expected because the pressure appears in the form of its gradient and is therefore only defined up to a constant in the first place. Indeed, the term in (2.13) proportional to γ is also not relevant and can be discarded. At the same time, this explains the, at first sight dubious, dimensional argument of the $\log(x^2+y^2)$ function.

Unlike p, the integrals for v or u are convergent (outside the source) and can be found without resorting to generalized functions. We have

$$\tilde{v}(y,k) = \frac{\pi S}{\rho_0}\mathrm{e}^{-|ky|}\left(\mathrm{sign}(y) + \mathrm{sign}(\mathrm{Re}\,k)\frac{\sigma}{\Omega_0}\right), \tag{2.14a}$$

$$\tilde{u}(y,k) = \frac{\mathrm{i}\pi S}{\rho_0}\mathrm{e}^{-|ky|}\left(\mathrm{sign}(\mathrm{Re}\,k) + \mathrm{sign}(y)\frac{\sigma}{\Omega_0}\right) \tag{2.14b}$$

and obtain

$$v(x,y) = \frac{S}{\rho_0}\frac{y}{x^2+y^2} - \frac{S\sigma}{2\rho_0U_0}\left[E(k_0,z) + E(k_0,\bar{z}) - 2\pi\mathrm{i}H(x)\mathrm{e}^{-\mathrm{i}k_0x-k_0|y|}\right], \tag{2.15a}$$

$$u(x,y) = \frac{S}{\rho_0}\frac{x}{x^2+y^2} + \frac{\mathrm{i}S\sigma}{2\rho_0U_0}\left[E(k_0,z) - E(k_0,\bar{z}) + 2\pi\mathrm{i}\,\mathrm{sign}(y)H(x)\mathrm{e}^{-\mathrm{i}k_0x-k_0|y|}\right]. \tag{2.15b}$$

The branch cuts of the exponential integrals (in the E-functions) cancel the jumps due to the $H(x)$-terms, to produce continuous p and v fields. Only u has a tangential discontinuity along $y=0, x>0$, but this is due to the $\mathrm{sign}(y)$ term. This corresponds with the $\delta(y)$-function behaviour of the vorticity given in (1.11).

2.2. *An example*

A typical example of this solution, in the form of iso-colour plots in the x–y plane of snapshots in time of the (real parts of) pressure and velocity fields (i.e. including the factor $\mathrm{e}^{\mathrm{i}\omega t}$), is given in figure 1. The parameters used are $\omega=8$, $\sigma=6$, $U_0=3$, and hence $k_0=2.667$. The values of σ and ω are taken of the same order of magnitude to include the effects of both shear and vortex shedding.

The size of the figure is chosen such that there are two or three vortices visible. The time (corresponding to a phase point $\omega t=\pi$) is the same in all figures.

In order to remove the effect of the undetermined constant, the plot-domain-averaged value of p is subtracted from p. The hydrodynamic wavelength is $2\pi/k_0=2.36$, corresponding in the figures to twice the length of the vorticity blobs. As expected, u is discontinuous across $y=0, x>0$, whereas v and p are continuous everywhere (outside the source). The velocity fields are confined to the neighbourhoods of source and trailing vortices. Since $\omega\neq\sigma$, the pressure diverges logarithmically, indicating the generation of acoustic waves in a compressible far-field outer problem.

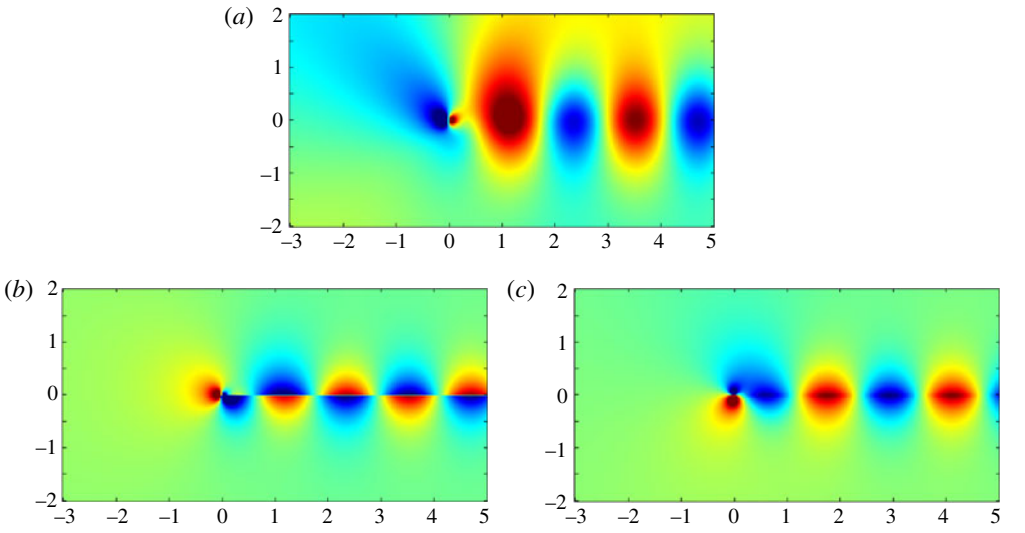

FIGURE 1. (Colour online) See § 2.2. Iso-colour plots of the (real parts of) pressure and velocities for a typical free-field case in the x–y plane as snapshots in time. $\omega = 8$, $\sigma = 6$, $U_0 = 3$, giving $k_0 = 2.67$: (*a*) pressure; (*b*) u-velocity; (*c*) v-velocity.

2.3. *Interpretation for compressible duct flow*

For a comparison with the three-dimensional acoustic problem of a cylindrical duct of radius a, mean flow of Mach number M and boundary layer thickness ah as considered by Brambley *et al.* (2012), we note that in the shear layer we have (in dimensionless form)

$$U(r) = Mh^{-1}(1 - r) = Mh^{-1}(1 - r_0) + Mh^{-1}(r_0 - r) \tag{2.16}$$

which is equivalent to the two-dimensional problem if we identify $y = a(r_0 - r)$, $U_0 = c_0M(1 - r_0)/h$, and $\sigma = c_0M/ah$ and $\omega := \omega c_0/a$, such that the dimensionless duct equivalent of k_0 is

$$k_0 := k_0 a = \frac{a\omega}{U_0} = \frac{\omega h}{M(1 - r_0)}. \tag{2.17}$$

Exactly the same trailing vorticity wavenumber k_0 is found in the acoustic duct problem as in the present two-dimensional incompressible problem. In the next section we will show that this analogy extends to the configuration where the source is positioned near an impedance wall. We will show that the surface waves excited in the incompressible problem have a clear and strict counterpart among the modes of the acoustic duct problem.

3. A time-harmonic line mass source in linear shear over an impedance wall

3.1. *The soft wall*

Consider the same equations (2.2) as before, but now in a region $y \in [0, \infty)$, with a source at $y = y_0$, and a wall of impedance $Z_w = \rho_0\zeta$ at $y = 0$ where U vanishes. We have, with $\Omega = \omega - kU$, $U(y) = U_0 + \sigma(y - y_0) = \sigma y$, $U_0 = \sigma y_0$, $\Omega_0 = \omega - kU_0$, $k_0 = \omega/U_0$ and $\tilde{p}(0) = -\rho_0\zeta\,\tilde{v}(0)$ at $y = 0$, the same incompressible Pridmore-Brown equation (2.3) and far-field conditions as for the free-field problem, but now with

boundary condition

$$\mathrm{i}\omega\tilde{p}(0) = \zeta\tilde{p}'(0). \tag{3.1}$$

Note that ζ has the dimension of velocity. Similarly to the free-field configuration, the Fourier-transformed solution can be constructed and is found to be

$$\begin{aligned}\tilde{p} = {} & \frac{\mathrm{i}\pi S}{|k|\Omega_0}\mathrm{e}^{-|k|y_>+|k|y_<}\big(\Omega_> - \operatorname{sign}(\operatorname{Re}k)\sigma\big)\big(\Omega_< + \operatorname{sign}(\operatorname{Re}k)\sigma\big)\\ & + \frac{\mathrm{i}\pi S}{|k|\Omega_0}\mathrm{e}^{-|k|y_>-|k|y_<}\big(\Omega_> - \operatorname{sign}(\operatorname{Re}k)\sigma\big)\big(\Omega_< - \operatorname{sign}(\operatorname{Re}k)\sigma\big)\\ & \times\frac{\mathrm{i}k\zeta + \sigma + \operatorname{sign}(\operatorname{Re}k)\omega}{\mathrm{i}k\zeta + \sigma - \operatorname{sign}(\operatorname{Re}k)\omega}\end{aligned} \tag{3.2}$$

where $y_< = \min(y, y_0)$, $y_> = \max(y, y_0)$ and $\Omega_{<>} = \Omega(y_{<>})$. We distinguish the incident and reflected parts:

$$\tilde{p} = \tilde{p}_{in} + \tilde{p}_{ref}, \tag{3.3a}$$

$$\tilde{p}_{in} = \frac{\mathrm{i}\pi S}{|k|\Omega_0}\mathrm{e}^{-|k||y-y_0|}(\Omega\Omega_0 - \sigma^2|k||y-y_0| - \sigma^2), \tag{3.3b}$$

$$\begin{aligned}\tilde{p}_{ref} = {} & \frac{\mathrm{i}\pi S}{|k|\Omega_0}\mathrm{e}^{-|k|(y+y_0)}(\Omega - \operatorname{sign}(\operatorname{Re}k)\sigma)(\Omega_0 - \operatorname{sign}(\operatorname{Re}k)\sigma)\\ & \times\frac{\mathrm{i}k\zeta + \sigma + \operatorname{sign}(\operatorname{Re}k)\omega}{\mathrm{i}k\zeta + \sigma - \operatorname{sign}(\operatorname{Re}k)\omega}.\end{aligned} \tag{3.3c}$$

A warning is in order here, that this split may imply the false suggestion that $\tilde{p}$ is singular at $k = 0$. In reality the singularities of $\tilde{p}_{in}$ and $\tilde{p}_{ref}$ cancel each other, at least when ζ is finite. In that case we have

$$\tilde{p} = 2\pi S(\mathrm{i}\omega y_< + \zeta) + O(k) \quad \text{for } k \to 0. \tag{3.4}$$

As a result the physical field p does not diverge for large $x^2 + y^2$, and there is no undetermined constant. In the hard-wall case ($\zeta \to \infty$), on the other hand, we still have a singularity at $k = 0$, while the physical field diverges and is determined only up to a constant. Note that all this agrees correctly with the role of p in the boundary condition: a soft-wall condition contains p explicitly, but in the hard-wall condition we have only its derivative.

As before, the physical field in the x, y-domain is obtained by inverse Fourier transformation,

$$p(x, y) = \frac{1}{2\pi}\int_{-\infty}^{\infty}\tilde{p}(y, k)\mathrm{e}^{-\mathrm{i}kx}\,\mathrm{d}k = p_{in} + p_{ref}, \tag{3.5}$$

with a pole at $k = k_0$ (the vorticity shed from the source), and possibly at one or two locations $k = k_s$ given by the dispersion relation for surface-wave-like modes

$$k_s = \mathrm{i}\zeta^{-1}\left(\sigma - \operatorname{sign}(\operatorname{Re}k_s)\omega\right). \tag{3.6}$$

In particular, assuming that $\sigma > 0$ and $\omega > 0$, and noting that $\operatorname{Re}\zeta > 0$ on physical grounds, we may distinguish the following cases (see figure 2):

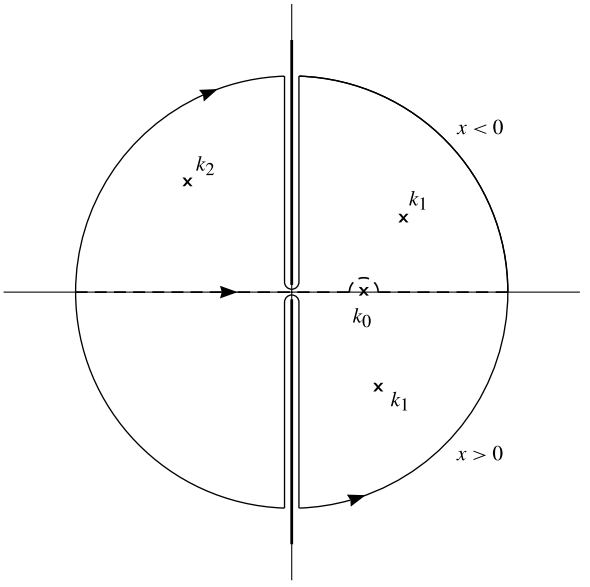

FIGURE 2. Complex k-plane with possible positions of poles, branch cuts of $|k|$, and original (- - -) and deformed (——) Fourier inversion contours for $x < 0$ and $x > 0$.

Case i.	Im $\zeta > 0$,	$\sigma > \omega$:	$k_s = k_1 \in$ 1st quadrant
Case ii.	Im $\zeta > 0$,	$\sigma \leqslant \omega$:	no k_s present
Case iii.	Im $\zeta < 0$,	$\sigma \geqslant \omega$:	$k_s = k_2 \in$ 2nd quadrant
Case iv.	Im $\zeta < 0$,	$\sigma < \omega$:	$k_s = k_1 \in$ 4th quadrant
			$k_s = k_2 \in$ 2nd quadrant

where

$$k_1 = \mathrm{i}\zeta^{-1}(\sigma - \omega), \quad k_2 = \mathrm{i}\zeta^{-1}(\sigma + \omega). \tag{3.7}$$

If $\mathrm{Im}(\zeta) = 0$, the k_s poles are located just on the imaginary axis, i.e. on the branch cut of $|k|$. In that case we have to take the limit $\mathrm{Im}(\zeta) \to 0$ from above or below, with either limit giving the same result. If $\omega = \sigma$, $k_1 = 0$ while there will be no contribution from this pole.

These modes are evidently the incompressible limit of the acoustic surface waves (Rienstra 2003)

$$k = \pm\mathrm{i}\omega\sqrt{\zeta^{-2} - c_0^{-2}} \simeq \pm\mathrm{i}\omega\zeta^{-1} \tag{3.8}$$

that exist for $\mathrm{Im}\,\zeta < 0$ and no flow. There is no such clear relation, however, with the incompressible limit of the surface waves along an impedance wall in a uniform mean flow with the Ingard–Myers condition, given by Rienstra (2003). This is indeed to be expected as we have an infinite shear layer in one case against a vanishing boundary layer in the other. If we rewrite (12) of Rienstra (2003) into the present notation (and

correct a typo), we obtain the dispersion relation

$$(k_\infty - k)^2 - \mathrm{i}(\zeta/U_\infty)k_\infty|k| = 0, \tag{3.9}$$

where $k_\infty = \omega/U_\infty$ and U_∞ is the uniform mean flow velocity. This equation has zero, two or four solutions (one in each quadrant) depending on $\operatorname{Im}\zeta/U_\infty$ being >2, $\leqslant 2$, and $\leqslant -2$ respectively. This is to be compared with the zero, one or two solutions, depending on the signs of $\operatorname{Im}\zeta$ and $\sigma - \omega$, for the present shear flow case.

Because of the presence of the mean flow, it is not immediately clear whether the k_s-modes are stable. However, a Briggs–Bers stability analysis (Briggs 1964; Bers 1983) shows that any k_s is a stable mode. In fact, we will show that, with $\zeta = \zeta(\omega)$, and $\omega = \omega(k)$ defined by dispersion relation (3.6), $\operatorname{Im}\omega$ is bounded from below by zero as a function of real k, and hence no instabilities (either absolute or convective) are possible. Indeed, if we have $k \in \mathbb{R}$, then

$$\operatorname{Im}\omega = |k|\operatorname{Re}\zeta(\omega). \tag{3.10}$$

For a passive liner with $\operatorname{Re}\zeta > 0$ for real ω, this shows that $\operatorname{Im}\omega = 0$ only if $k = 0$. Under reasonable assumptions of smoothness of $\zeta(\omega)$, $\operatorname{Im}\omega(k)$ is continuous and hence can only change sign once, namely at $k = 0$. However, it does not change sign, for the following reason. When $|\zeta(\omega)| \geqslant O(\omega)$ for $\omega \to \infty$ (a reasonable assumption if the impedance involves inertia effects), ζ must vanish for large k, and so $\lim_{k\to\pm\infty}\zeta(\omega) = 0$. Because of causality (Rienstra 2006), $1/\zeta$ must be analytic in $\operatorname{Im}\omega < 0$ and so any zero of ζ has a positive imaginary part. So $\lim_{k\to\pm\infty}\operatorname{Im}\omega(k)$ is always positive, and in particular $\operatorname{Im}\omega$ is positive on either side of $k = 0$ and therefore does not change sign. Hence, $\min_{k\in\mathbb{R}}(\operatorname{Im}\omega) = 0$. Since this minimum is not negative, the modes are not unstable.

We continue with our construction of an explicit expression for p by noting that p_{in} is the same as for the free field, with y replaced by $y - y_0$, and we denote this free-field pressure by p_f (with a similar notation for the velocities). The reflected field is a contribution of the k_0 pole, any k_s poles present, and the branch cut integrals. The contribution from k_0 is only present downstream ($x > 0$). If we close the integral via $-\mathrm{i}\infty$ we capture the k_0-residue of p_{ref}

$$-\frac{\pi S\sigma^2}{\omega}(1 + k_0(y - y_0))\frac{k_0 - k_2}{k_0 - k_1}H(x)\mathrm{e}^{-\mathrm{i}k_0\bar{z}_+} \tag{3.11}$$

(where $z_\pm = x + \mathrm{i}(y \pm y_0)$) representing something like the image field of the shed vorticity. For the contributions from k_s poles we have to consider different cases, according to the possible positions of the k_s poles (see below).

Folding the integration contour around the branch cuts (see figure 2), we obtain integrals of the following type (derived in the same way as for (2.13), and with the branch cuts of E still to be determined):

$$\begin{aligned}\int_0^\infty \frac{(\lambda + p_1)(\lambda + p_2)(\lambda + p_3)}{\lambda(\lambda - \mathrm{i}q_1)(\lambda - \mathrm{i}q_2)}\mathrm{e}^{-\lambda z}\,\mathrm{d}\lambda = \frac{1}{z} + \frac{p_1p_2p_3}{q_1q_2}(\gamma + \log z)\\ - \frac{(p_1 + \mathrm{i}q_1)(p_2 + \mathrm{i}q_1)(p_3 + \mathrm{i}q_1)}{q_1(q_1 - q_2)}E(q_1, z)\\ - \frac{(p_1 + \mathrm{i}q_2)(p_2 + \mathrm{i}q_2)(p_3 + \mathrm{i}q_2)}{q_2(q_2 - q_1)}E(q_2, z).\end{aligned} \tag{3.12}$$

Altogether we can construct for the various cases explicit results, depending on the locations of the k_s poles. In general the pressure looks like

$$\begin{aligned} p(x,y) = p_f(x,y-y_0) - S\sigma y\frac{x}{x^2+(y+y_0)^2} - \frac{\mathrm{i}S}{\omega}(\sigma^2-\omega^2)\left[\gamma + \tfrac{1}{2}\log\left(x^2+(y+y_0)^2\right)\right] \\ - \frac{\mathrm{i}S\sigma^2}{2\omega}\left[(1-k_0(y-y_0))\frac{k_0-k_1}{k_0-k_2}E(k_0,z_+)\right. \\ \left. + (1+k_0(y-y_0))\frac{k_0-k_2}{k_0-k_1}\left(E(k_0,\bar{z}_+) - 2\pi\mathrm{i}H(x)\mathrm{e}^{-\mathrm{i}k_0\bar{z}_+}\right)\right] \\ + \frac{Sk_0}{\zeta}\left[\frac{k_1(U_0-\mathrm{i}\zeta)}{k_0-k_1}(\sigma y-\mathrm{i}\zeta)\left(E(k_1,\bar{z}_+)-C_1\right)\right. \\ \left. + \frac{k_2(U_0+\mathrm{i}\zeta)}{k_0-k_2}(\sigma y+\mathrm{i}\zeta)\left(E(k_2,z_+)-C_2\right)\right] \end{aligned} \tag{3.13}$$

where C_1 and C_2, given below, relate to the possible contributions of the poles k_1 and k_2. As noted above, this p is not divergent for large x^2+y^2 and has no undetermined constant. The terms with γ and log appear in both p_f and p_{ref} and cancel each other.

Using similar reasoning as before, this time without divergent integrals, we obtain from

$$\tilde{v}_{ref} = \frac{\pi S}{\rho_0}\mathrm{e}^{-|k|(y+y_0)}\left(1-\mathrm{sign}(\mathrm{Re}\,k)\frac{\sigma}{\Omega_0}\right)\frac{\mathrm{i}k\zeta+\sigma+\mathrm{sign}(\mathrm{Re}\,k)\omega}{\mathrm{i}k\zeta+\sigma-\mathrm{sign}(\mathrm{Re}\,k)\omega}, \tag{3.14a}$$

$$\tilde{u}_{ref} = \frac{\mathrm{i}\pi S}{\rho_0}\mathrm{e}^{-|k|(y+y_0)}\left(\mathrm{sign}(\mathrm{Re}\,k)-\frac{\sigma}{\Omega_0}\right)\frac{\mathrm{i}k\zeta+\sigma+\mathrm{sign}(\mathrm{Re}\,k)\omega}{\mathrm{i}k\zeta+\sigma-\mathrm{sign}(\mathrm{Re}\,k)\omega} \tag{3.14b}$$

the velocities

$$\begin{aligned} v(x,y) = v_f(x,y-y_0) + \frac{S}{\rho_0}\frac{y+y_0}{x^2+(y+y_0)^2} \\ + \frac{S\sigma}{2\rho_0U_0}\left[\frac{k_0-k_1}{k_0-k_2}E(k_0,z_+) + \frac{k_0-k_2}{k_0-k_1}\left(E(k_0,\bar{z}_+) - 2\pi\mathrm{i}H(x)\mathrm{e}^{-\mathrm{i}k_0\bar{z}_+}\right)\right] \\ + \frac{\mathrm{i}Sk_0}{\rho_0\zeta}\left[\frac{k_1(U_0-\mathrm{i}\zeta)}{k_0-k_1}\left(E(k_1,\bar{z}_+)-C_1\right) + \frac{k_2(U_0+\mathrm{i}\zeta)}{k_0-k_2}\left(E(k_2,z_+)-C_2\right)\right], \end{aligned} \tag{3.15}$$

$$\begin{aligned} u(x,y) = u_f(x,y-y_0) + \frac{S}{\rho_0}\frac{x}{x^2+(y+y_0)^2} \\ - \frac{\mathrm{i}S\sigma}{2\rho_0U_0}\left[\frac{k_0-k_1}{k_0-k_2}E(k_0,z_+) - \frac{k_0-k_2}{k_0-k_1}\left(E(k_0,\bar{z}_+) - 2\pi\mathrm{i}H(x)\mathrm{e}^{-\mathrm{i}k_0\bar{z}_+}\right)\right] \\ - \frac{Sk_0}{\rho_0\zeta}\left[\frac{k_1(U_0-\mathrm{i}\zeta)}{k_0-k_1}\left(E(k_1,\bar{z}_+)-C_1\right) - \frac{k_2(U_0+\mathrm{i}\zeta)}{k_0-k_2}\left(E(k_2,z_+)-C_2\right)\right]. \end{aligned} \tag{3.16}$$

The contributions C_1 and C_2 are as follows.

Case i (1 pole). $k_s = k_1$ is found in the upper half-plane and therefore contributes upstream:

$$C_1 = -2\pi\mathrm{i}H(-x)\mathrm{e}^{-\mathrm{i}k_1\bar{z}_+}, \quad C_2 = 0. \tag{3.17a}$$

Case ii (no pole). No k_s pole present, so

$$C_1 = 0, \quad C_2 = 0. \tag{3.17b}$$

Case iii (1 pole). $k_s = k_2$ is found in the upper half-plane and contributes upstream:

$$C_1 = 0, \quad C_2 = 2\pi \mathrm{i} H(-x)\mathrm{e}^{-\mathrm{i}k_2 z_+}. \tag{3.17c}$$

Case iv (2 poles). One $k_s = k_1$ is now found in the lower half-plane and contributes downstream, while a second $k_s = k_2$, and therefore C_2, is the same as in case iii above. We have

$$C_1 = 2\pi \mathrm{i} H(x)\mathrm{e}^{-\mathrm{i}k_1 \bar{z}_+}, \quad C_2 = 2\pi \mathrm{i} H(-x)\mathrm{e}^{-\mathrm{i}k_2 z_+}. \tag{3.17d}$$

The exponential integral E_1 in the function $E(q, z)$, $q \in \mathbb{C}$, defined in (A 3) in the Appendix, does not follow the standard definition anymore. Instead of a branch cut along the negative real axis of the argument, the branch cut is rotated and depends on q in such a way that if $\mathrm{Re}(q) > 0$, the branch cut of $E_1(-\mathrm{i}qz)$ is always mapped along the line $x = 0, y < 0$, and thus for $E_1(-\mathrm{i}q\bar{z})$ is the branch cut located along the line $x = 0, y > 0$; if $\mathrm{Re}(q) < 0$ it is the other way round (see the Appendix for more details). This definition only differs from the standard one if q is not both real and positive, and therefore agrees with $E(k_0, z)$ in (2.13).

As for the free-field problem, the branch cuts of the E functions now compensate for the jumps of the Heaviside functions, which were not physical but were artefacts of the contour being closed via the lower (if $x > 0$) or upper (if $x < 0$) complex half-plane. The resulting fields are therefore smooth and continuous apart from the discontinuity in u due to the sign(y) term in the free-field solution u_f mentioned previously.

3.2. *The hard-wall limit*

A special case of interest is the hard-wall limit, i.e. $\zeta \to \infty$. This limit is relatively easily found for the velocities. They show a certain symmetry about $y = 0$:

$$\begin{aligned} v_{HW}(x, y) = {} & \frac{S}{\rho_0} \frac{y - y_0}{x^2 + (y - y_0)^2} - \frac{S\sigma}{2\rho_0 U_0} \left[E(k_0, z_-) + E(k_0, \bar{z}_-) - 2\pi \mathrm{i} H(x)\mathrm{e}^{-\mathrm{i}k_0 x - k_0 |y - y_0|} \right] \\ & - \left(\frac{S}{\rho_0} \frac{-(y + y_0)}{x^2 + (y + y_0)^2} - \frac{S\sigma}{2\rho_0 U_0} \left[E(k_0, \bar{z}_+) + E(k_0, z_+) - 2\pi \mathrm{i} H(x)\mathrm{e}^{-\mathrm{i}k_0 x - k_0 (y + y_0)} \right] \right), \end{aligned} \tag{3.18}$$

$$\begin{aligned} u_{HW}(x, y) = {} & \frac{S}{\rho_0} \frac{x}{x^2 + (y - y_0)^2} + \frac{S}{\rho_0} \frac{x}{x^2 + (y + y_0)^2} \\ & + \frac{\mathrm{i}S\sigma}{2\rho_0 U_0} \left[E(k_0, z_-) - E(k_0, \bar{z}_-) + 2\pi \mathrm{i} \,\mathrm{sign}(y - y_0) H(x)\mathrm{e}^{-\mathrm{i}k_0 x - k_0 |y - y_0|} \right] \\ & + \frac{\mathrm{i}S\sigma}{2\rho_0 U_0} \left[E(k_0, \bar{z}_+) - E(k_0, z_+) + 2\pi \mathrm{i} \,\mathrm{sign}(-(y + y_0)) H(x)\mathrm{e}^{-\mathrm{i}k_0 x - k_0 (y + y_0)} \right]. \end{aligned} \tag{3.19}$$

As a result, the expressions can be written in terms of the free-field velocities as follows:

$$v_{HW}(x, y) = v_f(x, y - y_0) - v_f(x, -(y + y_0)), \tag{3.20a}$$

$$u_{HW}(x, y) = u_f(x, y - y_0) + u_f(x, -(y + y_0)). \tag{3.20b}$$

The hard-wall limit for pressure, on the other hand, is more subtle than may be expected, because it contains (like the free-field solution) an inherent undetermined additive constant, in contrast to the soft-wall solution. A limit of large ζ is therefore not straightforward and it seems better to derive the solution directly from the Fourier

integral representation. We have

$$\tilde{p}_{ref} = \frac{\mathrm{i}\pi S}{|k|\Omega_0}\mathrm{e}^{-|k|(y+y_0)}(\Omega - \mathrm{sign}(\mathrm{Re}\,k)\sigma)(\Omega_0 - \mathrm{sign}(\mathrm{Re}\,k)\sigma) \tag{3.21}$$

which yields for $x > 0$ a contribution from the k_0-pole

$$-\frac{\pi S\sigma^2}{\omega}(1 + k_0(y - y_0))H(x)\mathrm{e}^{-\mathrm{i}k_0\bar{z}_+}. \tag{3.22}$$

For the contributions from the branch cuts we follow the same procedure as before, using the auxiliary result (valid whenever the integral converges)

$$\int_0^\infty \frac{(z+p_1)(z+p_2)}{z(z-\mathrm{i}q)}\mathrm{e}^{-\lambda z x}\,\mathrm{d}\lambda = \frac{1}{x} - \mathrm{i}\frac{p_1 p_2}{q}(\gamma + \log x) - \mathrm{i}\frac{1}{q}(p_1 + \mathrm{i}q)(p_2 + \mathrm{i}q)E(q, x) \tag{3.23}$$

to obtain

$$\begin{aligned} p_{HW}(x, y) = {} & p_f(x, y - y_0) - S\sigma y\frac{x}{x^2 + (y + y_0)^2} \\ & - \mathrm{i}\frac{S}{2\omega}\left[(\sigma + \omega)^2\left(\gamma + \mathrm{Log}(-\mathrm{i}z_+)\right) + (\sigma - \omega)^2\left(\gamma + \mathrm{Log}(\mathrm{i}\bar{z}_+)\right)\right] \\ & - \mathrm{i}\frac{S\sigma^2}{2\omega}[(1 - k_0(y - y_0))E(k_0, z_+) \\ & + (1 + k_0(y - y_0))(E(k_0, \bar{z}_+) - 2\pi\mathrm{i}H(x)\mathrm{e}^{-\mathrm{i}k_0\bar{z}_+})] \end{aligned} \tag{3.24}$$

valid for both $x > 0$ and $x < 0$, and where Log denotes the principal-value logarithm (see (A 3)). As before, the constants (like the terms with γ) can be discarded.

Indeed, if we take directly the limit $\zeta \to \infty$ of (3.13) but ignore the diverging $\log\zeta$-terms, we find the same result, apart of course from the additive constant.

Note that p_{HW} is, remarkably, not similar to the corresponding expressions (3.20) for the velocities.

3.3. *Examples*

In figures 3 and 4 graphical representations in the form of iso-colour plots in the x–y plane are given for the (real parts of) pressure and velocity fields along soft and hard walls for a number of typical cases: $\omega = 8$ combined with $\sigma = 6$ and $\sigma = 10$, and hard walls compared with soft walls of $\zeta = 4 - 2\mathrm{i}$, corresponding to a case iii and a case iv. This value of ζ is selected to be of the order of magnitude of U_0. The variation in σ has a significant effect. However, taking $\zeta = 4 + 2\mathrm{i}$, corresponding to case i and case ii situations, does not give significantly different results and is therefore not shown here. Again the effect of the undetermined constant in p for the hard-wall case is removed by subtracting its plot-domain-averaged value. The time (corresponding to a phase point $\omega t = \pi$) is the same in all figures.

The parameters chosen for figure 3 are $\omega = 8$, $y_0 = 0.5$, $\sigma = 6$, and hence $U_0 = 3$, $k_0 = 2.67$, and $k_1 = 0.2 - 0.4\mathrm{i}$ and $k_2 = -1.4 + 2.8\mathrm{i}$ (case iv) for the soft wall. The hydrodynamic wavelength is $2\pi/k_0 = 2.36$, just large enough to have some interaction with the wall.

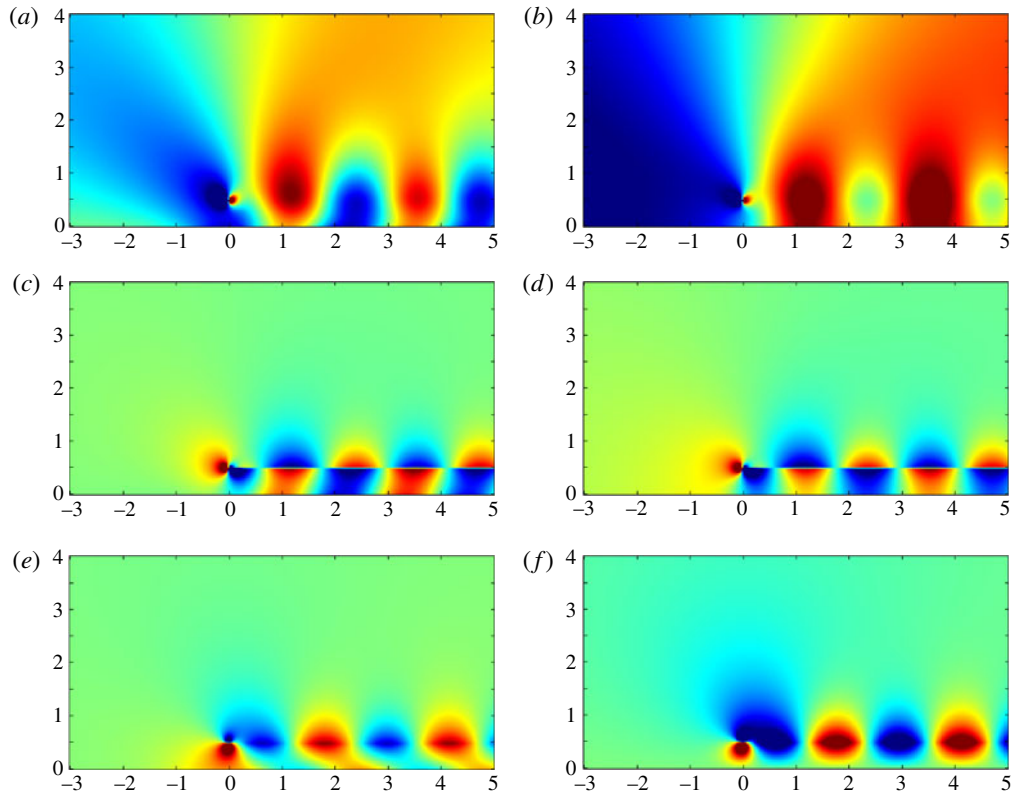

FIGURE 3. (Colour online) See § 3.3. Iso-colour plots in the x–y plane of a typical case with hard and soft walls along $y = 0$, as snapshots in time, of the (real parts of) pressure and velocities, when $\omega = 8$, $\sigma = 6$, $y_0 = 0.5$, giving $U_0 = 3$, $k_0 = 2.67$. For the soft wall: $\zeta = 4 - 2\mathrm{i}$, $k_1 = 0.2 - 0.4\mathrm{i}$, $k_2 = -1.4 + 2.8\mathrm{i}$ (case iv): (*a*) pressure, soft wall; (*b*) pressure, hard wall; (*c*) u-velocity, soft wall; (*d*) u-velocity, hard wall; (*e*) v-velocity, soft wall; (*f*) v-velocity, hard wall.

The parameters chosen for figure 4 are $\omega = 8$, $y_0 = 0.5$, $\sigma = 10$, and hence $U_0 = 5$, $k_0 = 1.6$, and $k_1 = -0.2 + 0.4\mathrm{i}$ and $k_2 = -1.8 + 3.6\mathrm{i}$ (case iii) for the soft wall. The hydrodynamic wavelength $2\pi/k_0 = 3.93$ is now large compared to the wall distance $y_0 = 0.5$. This results into a strong interaction of the shed vorticity field with the wall, especially for the velocities.

3.4. *Interpretation for acoustic duct modes with lined walls*

In order to compare with the acoustic problem of a lined flow duct, we note that $\rho_0\zeta = \rho_0 c_0 Z$ such that the dimensionless duct equivalents of k_s are

$$k_s := k_s a = \frac{\mathrm{i}}{Z}\left(\frac{M}{h} \pm \omega\right). \tag{3.25}$$

These do indeed correspond to two of the compressible surface modes, as is clearly seen in figure 5. We use the notation and geometry of Brambley *et al.* (2012), i.e. a

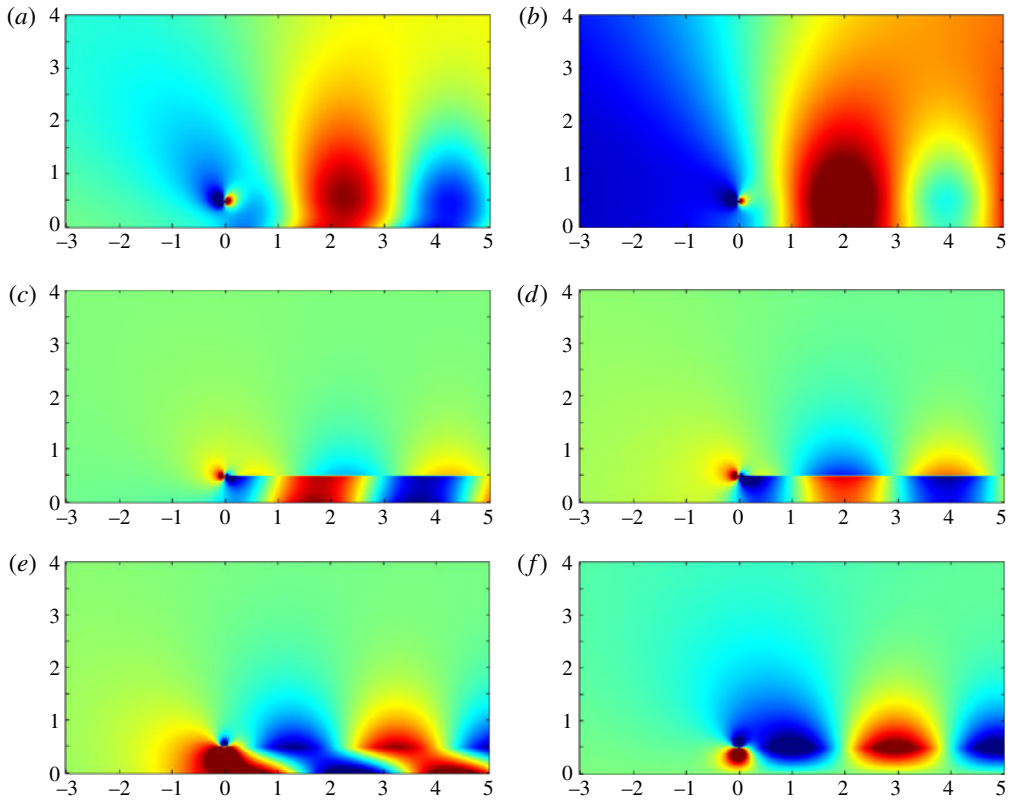

FIGURE 4. (Colour online) See § 3.3. Iso-colour plots in the x–y plane of a typical case with hard and soft walls along $y = 0$, as snapshots in time, of the (real parts of) pressure and velocities, when $\omega = 8$, $\sigma = 10$, $y_0 = 0.5$, giving $U_0 = 5$, $k_0 = 1.6$. For the soft wall: $\zeta = 4 - 2\mathrm{i}$, $k_1 = -0.2 + 0.4\mathrm{i}$, $k_2 = -1.8 + 3.6\mathrm{i}$ (case iii): (*a*) pressure, soft wall; (*b*) pressure, hard wall; (*c*) u-velocity, soft wall; (*d*) u-velocity, hard wall; (*e*) v-velocity, soft wall; (*f*) v-velocity, hard wall.

cylindrical duct with linear-then-constant mean flow

$$U(r) = \begin{cases} M, & 0 \leqslant r \leqslant 1 - h, \\ M(1 - r)/h, & 1 - h \leqslant r \leqslant 1, \end{cases} \tag{3.26}$$

with M the mean flow Mach number.

It should be noted that the surface modes k_+ and k_- found by Brambley *et al.* (2012) and shown in figure 5 around $k = 70$ do not have incompressible infinite-shear counterparts, suggesting that the physics causing them may be significantly different from the physics causing the k_0-pole despite their similar locations in the k-plane.

4. Conclusions

The analytically exact and explicit solutions for the problem of a time-harmonic line mass source in incompressible inviscid two-dimensional linear shear mean flow are derived for the free-field situation and for a semi-infinite space with the mean flow directed parallel to and vanishing at an impedance wall. Both problems were motivated

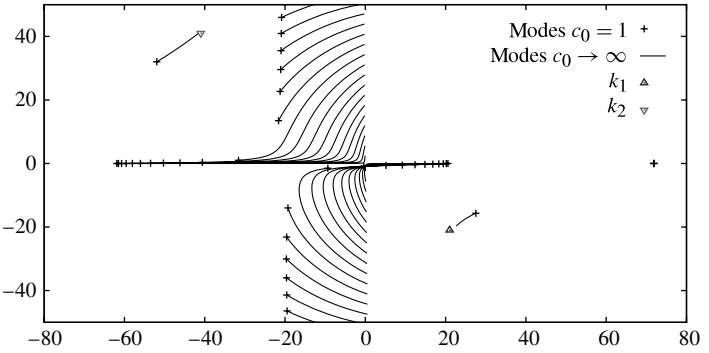

FIGURE 5. Tracking the k_1 and k_2 surface modes in a three-dimensional duct, for a medium turning from fully compressible to incompressible. A case iv parameter choice is shown, with $\omega = 31$, $m = 0$, $U_0 = 0.5$, $h = 0.05$, $Z = 0.5 - 0.5\mathrm{i}$ (scaled on ρ_0). k_0 depends on source position r_0 and is not drawn.

by the problem of an acoustic source in a shear flow along a lined wall, for example a boundary layer.

Both solutions were obtained by Fourier transformation in the mean flow direction x, which leads to equations in the cross-wise direction y that are solvable exactly (Rayleigh 1945; Drazin & Reid 2004). The inverse transform of the pressure, however, leads for the free-field and the hard-wall problems to divergent integrals because of logarithmic behaviour of the far field of a line source in two-dimensional incompressible flow. This behaviour is well-known in uniform or vanishing mean flow conditions, but appears to exist also in shear flow unless the shear parameter σ is exactly equal to the frequency ω. In a more comprehensive compressible context, this divergence does not exist. In a small Helmholtz and Mach number setting of matched asymptotic expansions, the far field of the incompressible 'inner' problem would match with a decaying compressible 'outer field' like in Wu (2002); see also Lesser & Crighton (1975) and Crighton *et al.* (1992). Apart from its physical relevance, the divergent integral is not insurmountable and can be cured by interpreting the integrals in a generalized sense.

The dominating feature in the solutions found is a non-decaying train of vortices, shed from the line source (possibly comparable with a von Kármán vortex street). This trailing vorticity field is essentially due to the mean flow shear. In an irrotational mean flow, a line source would not generate vorticity, as shown in (1.3); generating vorticity in an irrotational mean flow would require at least a force.

Since with hard-wall conditions the pressure appears only in the form of its gradient while it has no natural conditions at infinity, this variable is only determined up to an undetermined constant, so care is needed when the hard-wall limit is taken from the soft-wall solution. In general, it seems better to derive the solution directly from the Fourier integral, albeit via divergent integrals. All this is not the case with the velocity. Here the natural conditions at infinity are a vanishing velocity, such that the method of Fourier transformation automatically sifts out the required solution.

In a compressible context, this work identifies the k_0-pole found by Brambley *et al.* (2012) as shed vorticity from the point source, as was speculated. However, this work also shows that the possibly related surface modes k_+ and k_- found by Brambley *et al.* (2012) are not present here and therefore do not have incompressible infinite-shear

counterparts, suggesting that the physics causing them may be significantly different from the physics causing the k_0-pole despite their similar locations in the k-plane. As shown in figure 5, the two surface modes that do occur here correspond to another two of the possible six compressible surface modes for compressible shear flow over a lining (Brambley 2011).

Acknowledgements

A preliminary version of this work (Brambley, Darau & Rienstra 2011) was presented as part of paper AIAA-2011-2806 at the 17th AIAA/CEAS Aeroacoustics Conference.

M.D.'s contribution was part of PhD work in a cooperation between TU Eindhoven (Netherlands) and the West University of Timişoara (Romania), supervised by Professors R. R. M. Mattheij and S. Balint. She acknowledges the support by a grant of the Romanian National Authority for Scientific Research, CNCS-UEFISCDI, project number PN-II-ID-PCE-2011-3-0171. E.J.B. was supported by a Research Fellowship at Gonville & Caius College, Cambridge. We thank G.-J. van Heijst and L. Kamp for their insightful remarks regarding vortex stretching. The referees are thanked for their helpful comments and useful suggestions, which have led to improvement of the work.

Appendix. The exponential integral

An important function in the foregoing analysis is the function $E(q, z)$, closely related to the exponential integral E_1 (Abramowitz & Stegun 1965, equation (5.1.1)). For $q, z \in \mathbb{C}$, but with the branch cut for E_1 yet to be selected, we have

$$E(q, z) = \mathrm{e}^{-\mathrm{i}qz} E_1(-\mathrm{i}qz), \tag{A 1a}$$

$$E_1(z) = \int_z^\infty \frac{\mathrm{e}^{-t}}{t}\,\mathrm{d}t = -\gamma - \log z + \sum_{k=1}^{\infty} \frac{(-1)^{k+1} z^k}{k\,k!}, \tag{A 1b}$$

where $\gamma = 0.5772156649\ldots$ is Euler's constant. The variable q corresponds here to complex wavenumbers (k_0 and k_s), while $z = x + \mathrm{i}y$ relates to the physical (x, y)-space. As is clear from the series representation, $E_1(z)$ has a logarithmic singularity, for which the standard definition is to use the principal value, Log, with $\mathrm{Log}(1) = 0$ and a branch cut along the negative real axis. However, with our applications this choice would result in q-dependent branch cuts in the x, y-domain and is therefore not convenient.

The branch cut discontinuity is the counterpart of the discontinuity at the line $x = 0$ due to the upward or downward closure of the Fourier integral contour for $x < 0$ or $x > 0$ respectively. Therefore, a most natural location for the branch cut is the imaginary axis.

The choice used here is such that if $\mathrm{Re}\, q > 0$ the branch cut of $E(q, z)$ is along the line $x = 0, y < 0$ and thus for $E(q, \bar{z})$ along the line $x = 0, y > 0$. If $\mathrm{Re}\, q < 0$ it is the opposite: the branch cut of $E(q, z)$ is then taken along the line $x = 0, y > 0$. This is most easily obtained by the logarithm

$$\log(-\mathrm{i}qz) \overset{\mathrm{def}}{=} \mathrm{Log}\left(-\mathrm{i}z\frac{q}{|q|}\right) + \mathrm{Log}(|q|) \tag{A 2}$$

with the principal value Log and $|q|$ as defined in (2.5). So we define, with this log and E_1 the standard exponential integral, our function E as

$$E(q,z) \overset{\text{def}}{=} \mathrm{e}^{-\mathrm{i}qz}\left(E_1(-\mathrm{i}qz) + \mathrm{Log}(-\mathrm{i}qz) - \mathrm{Log}\left(-\mathrm{i}z\frac{q}{|q|}\right) - \mathrm{Log}(|q|)\right). \qquad (A\,3)$$

REFERENCES

ABRAMOWITZ, M. & STEGUN, I. A. 1965 *Handbook of Mathematical Functions*. Dover.

BALSA, T. F. 1988 On the receptivity of free shear layers to two-dimensional external excitation. *J. Fluid Mech.* **187**, 155–177.

BERS, A. 1983 Space–time evolution of plasma instabilities – absolute and convective. In *Handbook of Plasma Physics: Volume 1 Basic Plasma Physics* (ed. A.A. Galeev & R.N. Sudan). pp. 451–517. North Holland, chap. 3.2.

BRAMBLEY, E. J. 2011 Surface modes in sheared flow using the modified Myers boundary condition. *AIAA Paper* 2011–2736.

BRAMBLEY, E. J., DARAU, M. & RIENSTRA, S. W. 2011 The critical layer in sheared flow. *AIAA Paper* 2011–2806.

BRAMBLEY, E. J., DARAU, M. & RIENSTRA, S. W. 2012 The critical layer in linear-shear boundary layers over acoustic linings. *J. Fluid Mech.* **710**, 545–568.

BRIGGS, R. J. 1964 *Electron-Stream Interaction with Plasmas*, *Monograph*, vol. 29. MIT.

CRIGHTON, D. G., DOWLING, A. P., FFOWCS WILLIAMS, J. E., HECKL, M. & LEPPINGTON, F. G. 1992 *Modern Methods in Analytical Acoustics. Lecture Notes*, Springer.

CRIMINALE, W. O. & DRAZIN, P. G. 1990 The evolution of linearized parallel flows. *Stud. Appl. Maths* **83**, 123–157.

CRIMINALE, W. O. & DRAZIN, P. G. 2000 The initial-value problem for a modeled boundary layer. *Phys. Fluids* **12** (2), 366–374.

DRAZIN, P. G. & REID, W. H. 2004 *Hydrodynamic Stability*, 2nd edn. Cambridge University Press.

GOLDSTEIN, M. E. & LEIB, S. J. 2005 The role of instability waves in predicting jet noise. *J. Fluid Mech.* **525**, 37–72.

JONES, D. S. 1982 *The Theory of Generalised Functions*, 2nd edn. Cambridge University Press.

KUNDU, P. K. & COHEN, I. M. 2002 *Fluid Mechanics*. Academic.

LESSER, M. B. & CRIGHTON, D. G. 1975 Physical acoustics and the method of matched asymptotic expansions. In *Physical Acoustics* (ed. W.P. Mason & R.N. Thurston). vol. XI. Academic.

PRIDMORE-BROWN, D. C. 1958 Sound propagation in a fluid flowing through an attenuating duct. *J. Fluid Mech.* **4**, 393–406.

RAYLEIGH, J. W. S. 1945 *Theory of Sound*, vol. II. Dover.

RIENSTRA, S. W. 2003 A classification of duct modes based on surface waves. *Wave Motion* **37** (2), 119–135.

RIENSTRA, S. W. 2006 Impedance models in time domain, including the extended Helmholtz resonator model. *AIAA Paper* 2006–2686.

SUZUKI, T. & LELE, S. K. 2003*a* Green's functions for a source in a mixing layer: direct waves, refracted arrival waves and instability waves. *J. Fluid Mech.* **477**, 89–128.

SUZUKI, T. & LELE, S. K. 2003*b* Green's functions for a source in a boundary layer: direct waves, channelled waves and diffracted waves. *J. Fluid Mech.* **477**, 129–173.

TENNEKES, H. & LUMLEY, J. L. 1972 *A First Course of Turbulence*. MIT.

WU, X. 2002 Generation of sound and instability waves due to unsteady suction and injection. *J. Fluid Mech.* **453**, 289–313.

WU, X. 2011 On generation of sound in wall-bounded shear flows: back action of sound and global acoustic coupling. *J. Fluid Mech.* **689**, 279–316.